

Neuroblastoma Cells Classification Through Learning Approaches by Direct Analysis of Digital Holograms

Mattia Delli Priscoli ¹, Pasquale Memmolo ¹, Gioele Ciaparrone ¹, Vittorio Bianco ¹, Francesco Merola ¹, Lisa Miccio, Francesco Bardozzo ², Daniele Pirone ², Martina Mugnano, Flora Cimmino, Mario Capasso, Achille Iolascon, Pietro Ferraro, *Senior Member, IEEE*, and Roberto Tagliaferri ¹, *Senior Member, IEEE*

Abstract—The label-free single cell analysis by machine and Deep Learning, in combination with digital holography in transmission microscope configuration, is becoming a powerful framework exploited for phenotyping biological samples. Usually, quantitative phase images of cells are retrieved from the reconstructed complex diffraction patterns and used as inputs of a deep neural network. However, the phase retrieval process can be very time consuming and prone to errors. Here we address the classification of cells by using learning strategies with images coming directly from the raw recorded digital holograms, i.e. without any data processing or refocusing involved. Indeed, in the raw digital hologram the entire complex amplitude information of the sample is intrinsically embedded in the form of modulated fringes. We develop a training strategy, based on deep and feature based machine learning models, in order to extract such information by skipping the classical reconstruction process for classifying different neuroblastoma cells. We provided an experimental validation by using the proposed strategy to classify two neuroblastoma cell lines.

Manuscript received December 3, 2020; revised February 3, 2021; accepted February 11, 2021. Date of publication February 19, 2021; date of current version October 6, 2021. This work was supported by PON-Programma Innovativo Nazionale Ricerca E Sviluppo 2014-2020. (Mattia Delli Priscoli, Pasquale Memmolo, Pietro Ferraro, and Roberto Tagliaferri contributed equally to this work.) (Corresponding author: Mattia DelliPriscoli.)

Mattia Delli Priscoli, Gioele Ciaparrone, Francesco Bardozzo, and Roberto Tagliaferri are with the Neurone Lab, Dep. of Management & Innovation Systems (DISA-MIS), University of Salerno, Via Giovanni Paolo II 132, Italy (e-mail: mdellipriscoli@unisa.it; gciaparrone@unisa.it; fbardozzo@unisa.it; rtagliaferri@unisa.it).

Pasquale Memmolo, Vittorio Bianco, Francesco Merola, Lisa Miccio, Martina Mugnano, and Pietro Ferraro are with the CNR-ISASI, Institute of Applied Sciences and Intelligent Systems “E. Caianiello,” Via Campi Flegrei 34, Pozzuoli, Napoli 80078, Italy (e-mail: p.memmolo@isasi.cnr.it; v.bianco@isasi.cnr.it; f.merola@isasi.cnr.it; lisa.miccio@isasi.cnr.it; m.mugnano@isasi.cnr.it; pietro.ferraro@cnr.it).

Daniele Pirone is with the CNR-ISASI, Institute of Applied Sciences and Intelligent Systems “E. Caianiello,” Via Campi Flegrei 34, Pozzuoli, Napoli 80078, Italy, and also with the Dipartimento di Ingegneria Elettrica e delle Tecnologie dell’ Informazione, Università di Napoli Federico II, Via Claudio 21, Napoli 80125, Italy (e-mail: danpir@virgilio.it).

Flora Cimmino is with the CEINGE Biotecnologie Avanzate, Via Comunale Margherita Napoli 484-538, Napoli 80131, Italy (e-mail: floracimmino81@gmail.com).

Mario Capasso and Achille Iolascon are with the CEINGE Biotecnologie Avanzate, Via Comunale Margherita Napoli 484-538, Napoli 80131, Italy, and also with the Dipartimento di Medicina Molecolare e Biotecnologie Mediche, Università di Napoli Federico II, 80131 Napoli, Italy (e-mail: mario.capasso@unina.it).

Color versions of one or more figures in this article are available at <https://doi.org/10.1109/JSTQE.2021.3059532>.

Digital Object Identifier 10.1109/JSTQE.2021.3059532

Index Terms—Artificial intelligence, supervised learning, machine learning, multilayer perceptrons, microfluidics, holography.

I. INTRODUCTION

DIGITAL holography (DH) in transmission microscope configuration has been successfully employed to the complete label-free analysis of biological samples thanks to the possibility to access to their quantitative phase-contrast information [1], [2]. In particular, phase images encode the coupling between the refractive index and the physical thickness of imaged cells, thus allowing the measure of three-dimensional (3D) morphometric features. Quantitative phase imaging provides highly informative content if compared to other imaging modalities, e.g., bright-field or fluorescence microscopy, allowing the calculation of unique cells characteristics [3]. A well-established analysis method to classify cells phenotyping relies on the joint use of features engineering and suitable classifiers, thus implementing conventional Machine Learning (ML) paradigms.

This has been exploited for blood cells characterization [4], sick cells identification [5], marine micro-organisms identification [3], just to name a few. Recently, a sub-class of ML, namely Deep Learning, has gained credits as the elective approach for advanced image analysis in microscopy [6]–[12]. DL employs multilayered convolutional neural networks (CNNs) to make the image features selection blind and automatic [13]. The combination of DL and DH in microscopy turned out to be decisive for a huge amount of applications, ranging from label-free classification [14] to advanced holographic image processing [15] with real-time performance. Usually, quantitative phase images of cells are retrieved from the reconstructed complex diffraction patterns and used as inputs of a deep CNN. Two main steps are needed to access the phase information from a digital hologram, i.e. the numerical refocusing [16], [17], and the corresponding phase calculation. The latter involves the extraction of the modulus 2π , or “wrapped” phase from the in-focus complex amplitude, and the phase unwrapping step. Numerical refocusing is typically an iterative method that estimates the best-focus distance to be set in the back-propagation kernel to reconstruct the sample in sharp focus. The wrapped phase images can be calculated by simple digital filtering in off-axis

recording scheme [18] or by a suitable iterative phase retrieval algorithm for in-line holograms [19]. Finally, phase unwrapping is a typically burdensome processing. Therefore, the whole phase reconstruction process is time consuming and the amplitude information is typically discarded. Thus, creating the large DH reconstructions dataset, required to train deep CNNs, can be very cumbersome and with long computational costs. Recently, a deep learning based approach has been used to overcome the problem. In fact, the entire holographic reconstruction process has been speeded up by solving an image-to-image regression problem for directly reconstructing the in-focus complex amplitude from the recorded hologram through a deep CNN [20]. However, it may take a long time for training in order to learn the reconstruction process and if the acquisition conditions were to change (different microscope objective or fringe patterning or CCD sensor), the training may be re-done.

Nowadays, many clinical tests are based on in-flow running of biological matter so that a long computational apparatus is not really workable when a decision-making is needed, for example in sorting devices. Indeed, in case of diagnostic strategies based on microfluidic systems, it would be a desirable configuration method working quasi real-time on flowing samples. Reducing the computational time, to obtain a preliminary phenotyping results, will be the route to pursue. In this framework, a raw digital hologram stores the complex amplitude of the sample in the form of a modulated fringe pattern. In principle, to associate an object to a certain population, its information does not really need to be decoded from the recorded pattern, provided that a suitable artificial intelligence model is properly trained with a fair number of examples. Based on this idea, in this paper we investigate the possibility to directly use raw recorded digital holograms for carrying out cells classification tasks through learning approaches, thus skipping the entire holographic reconstruction process without losing classification accuracy. Circulating tumor cells (CTCs) that originate from primary tumors spread to the bloodstream and become the source of metastasis. The detection of CTCs has been shown to be of prognostic value in the evaluation of cancer progression and for the study of the mechanisms of resistance to treatment [21]. Current methods of enrichment and isolation of CTCs depend on specific tumor antigens for the recognition of tumor cells [21]. Neuroblastoma has a high intra-tumor heterogeneity with different cells showing distinctive morphological and phenotypic profiles. Most liquid biopsy neuroblastoma studies referring to the detection of any tumor-derived material circulating in body fluids involved circulating tumor DNA or mRNA due to the universal and specific cell surface marker not available for CTCs. In this prospective study, we validate the proposed strategy by classifying two neuroblastoma cell lines, the CHP-134, consisting of the patient's tumor previously treated with chemotherapy and irradiation therapy and the SKNSH, established by primary bone marrow tumor. Digital holograms for the training dataset are obtained by recording flowing cells in a microfluidic channel. With the aim of augmenting the dataset, we induced controlled rolling to the cells [22], [23], thus having optical access to multiple views of the same cell. In this way, tens of cells per class have been recorded, each of them imaged with 80 – 100 different views.

The testing dataset is obtained by recording cells in a Petri dish thus obtaining hundreds of cells per class with few images.

Actually, the concept of direct classification without image reconstruction has been also investigated in other kinds of optical imaging systems and it can be implemented in diffractive imaging [24], scattering imaging [25] and single-pixel imaging [26]. In DH, the possibility to solve classification problems by using digital holograms as input of a learning-based classifier has been recently explored [27]–[29]. In particular, in ref. [27], the method named “ensemble deep learning invariant hologram classification” has been demonstrated for the classification of digital holograms of macroscopic objects, specifically handwritten digits. Instead, for the classification of holograms recorded in microscope configuration, the paper in [28] demonstrates, but only through a numerical simulations, the possibility to use neural networks in holographic flow cytometers for the classification of white blood cells. The work in [29] focuses on the classification of individual cells according to the number of cell-bound microbeads. It is based on the transfer learning exploiting a VGG19 pretrained network, which uses lensless in-line digital holograms of cells in a Petri dish as input. The approach we propose here, is based on the same concept expressed in [24]–[29] but it shows remarkable differences in terms of the type of input data, i.e. holograms of flowing cells for the training and static recording for the testing, and the classification tasks, i.e. phenotyping of CTCs. Concerning the learning method pipeline, leveraging Mask R-CNN, DH video frames and the recording cells in a Petri dish are segmented to reconstruct cells masks, used to build training, validation and test set. Then, those sets are used to fit Machine Learning (ML) and Deep Learning (DL) models to discriminate between the two neuroblastoma cell lines (CHP-134 and SK-N-SH). We demonstrate that using DL it is possible to correctly classify two neuroblastoma cell lines with an accuracy of 100%.

It is important to underline that the comparison among different learning strategies allows to identify a trade-off between the classification accuracy and the computational complexity of the selected learning method [30]. The paper is organized as follows. Section II presents the learning pipeline used to accomplish the classification task and describes the dataset used in this study. Section III presents the training procedures and a discussion of the experimental results. Finally, Section IV summarizes the work and the results obtained, and presents the future directions of research.

II. MATERIAL AND METHODS

The pipeline used to classify the cells consists of three main steps:

- First, DH video frames containing cells from the two cell lines are collected with two different methodologies. In-flow DH frames are used as training and validation sets, while DH frames collected on Petri dishes are used as test set. The in-flow frames give different views of the same cells, while the advantage of using Petri dishes is the ability to obtain many different cells in few frames, evaluating the robustness of the classifiers more accurately.

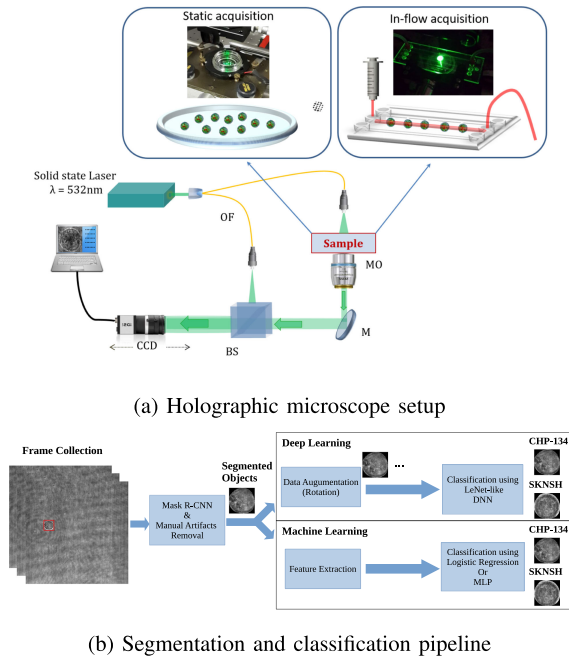


Fig. 1. (a) Schematic representation of the holographic microscope to acquire digital holograms of neuroblastoma cells in both static and continuous flow modalities. BS (beam splitter), MO (microscope objective), M (mirror), OF (optical fiber), CCD (Charge-Coupled Device); (b) The whole pipeline is summarized here. The holographic video frames (2048×2048 pixels) are collected. Then, using a Mask R-CNN, the cell masks are extracted from each frame. A visual refinement on the output masks is performed. The cells obtained from the segmentation process are then classified by a LeNet-like Deep Neural Network or by a ML feature based model into the two classes.

- Second, using transfer learning on COCO [31] dataset, a Mask R-CNN [32] model is trained on a subset of the training set cells. The Mask R-CNN is used to segment cells from both the in-flow video frames and the Petri dish images, in order to build the training, validation and test sets. A visual inspection is applied on the masks to remove the output False Positives.
- Finally, the single cells obtained in the previous step are fed to a binary classifier in order to discriminate between the two different neuroblastoma cell lines. Here we applied both feature-based ML algorithms and a DL model. In particular, we used a shallow Multilayer Perceptron (MLP) and Logistic Regression (LR) on a set of 10 manually extracted features [33]. For the DL approach we instead employed a LeNet-like CNN [34]. The CNN learned the features automatically during the training stage using an augmented dataset, which was obtained by rotating each cell 36 times, in order to obtain a rotationally invariant classifier (see Fig. 2).

Fig. 1 summarizes the entire pipeline implemented in this work, consisting of holographic images recording (Fig. 1(a)), the segmentation step using Mask R-CNN, manual refinement of the output masks and, finally, the classification step using feature-based ML algorithms and a DL model (Fig. 1(b)).

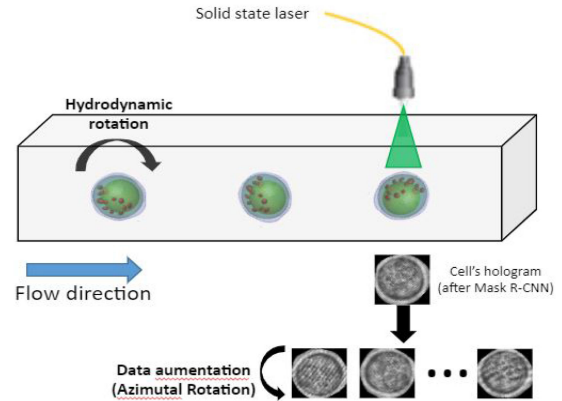


Fig. 2. Visual explanation about cell rotations. The Hydrodynamic forces, generated by a laminar flow in the microfluidic channel thus, inducing the cell's rotation within the imaged field of view. Once each cell is imaged, Mask RCNN extracts the foreground (the cells) from the background. After the recording step, data augmentation is applied to rotate the cell images azimuthally of 10 degrees 36 times.

A. Sample Preparation and Hologram Recording

Human neuroblastoma cell lines SK-N-SH and CHP-134 were chosen for analysis. SK-N-SH cells were cultured in Minimum Essential Medium (MEM) (Gibco-21090-022) supplemented with 10% fetal bovine serum, 2 mM L-glutamine and 100 U ml⁻¹ penicillin, 100 μ g ml⁻¹ streptomycin at 37°C in a CO₂ atm. CHP-134 were cultured in RPMI medium 1640 (Gibco-31870-025) supplemented with 10% fetal bovine serum, 2 mM L-glutamine and 100 U ml⁻¹ penicillin, 100 μ g ml⁻¹ streptomycin at 37°C in a CO₂ atm. Subsequently, they were harvested from the Petri dish by incubation with a 0.05% trypsin-EDTA solution (Sigma, St. Louis, MO) for 5 min. For the experiments in static condition, the cells were then centrifuged for 5 min at 1500 rpm, resuspended in complete medium and seeded in a WillCo-dish (WillCo-GWST-3522) at final concentration of 4×10^5 cells/ml. Instead, for in flow studies after centrifugation, the cells were resuspended in complete medium and injected into the microfluidic channel at final concentration of 4×10^5 cells/ml. To record digital holograms of neuroblastoma cells, we implement a classical digital holography (DH) microscope based on a Mach Zehnder interferometer. The light source is a 400 mW fiber coupled laser at 532 nm, whose beam is divided into a reference wave and an object wave and. The latter illuminates the sample within a microfluidic channel for the in-flow measurement and within a petri dish for the static acquisition. In particular, in the case of flowing cells, samples are inserted in a syringe activated by a controlled microfluidic pump with flux fixed at 7 nL/s and flows in a commercial microfluidic channel (PMMA polymeric material with cross section of $200 \mu\text{m} \times 200 \mu\text{m}$ and length 7 cm). In this condition, cells flow at an average velocity of 65 $\mu\text{m/s}$. Hydrodynamic forces, generated by a laminar flow in the microfluidic channel, induce cell's rotation within the imaged field of view, permitting to observe 80-100 different views of the same cell (see Fig. 2). After passing through a microscope objective (oil immersion 40 \times , numerical aperture 1.30, Plan Apochromat), the object wave interferes with the reference one in the beam

splitter. Finally, the interference fringe pattern, i.e. the digital hologram, propagates up to a 2048×2048 CCD camera (USB 3.0 u eye, from IDS), recording at 35 fps. In our experiments, we found cells flowing within a limited range, staying about $\pm 30 \mu\text{m}$ away from the observation plane. This permits to avoid severely unfocused objects. In Fig. 1 (a) reports the sketch of the holographic recording system, highlighting the two acquisition modalities, i.e. static and in continuous flow. We recorded digital hologram's time-laps of duration up to 5 minutes while cells are flowing and rotating along the microchannel.

B. Dataset Construction

The dataset consists of 12 in-flow DH video sequences for training and validation, from which a total of 21852 frames were extracted. The fringes visibility is optimized before each experiment in order to avoid sensitive intensity and contrast variations of fringes among holographic images of different video sequences. In each DH video sequence, cells belong to the same phenotype, therefore each detected cell is automatically labeled with the corresponding class. Moreover, in order to test the network generalization capabilities, 120 cells were recorded in Petri dish. The frames contained a variety of cancer cells belonging to two different types: CHP-134 and SK-N-SH, which we aim to classify using CNN and ML approaches. In Fig. 3 the in-flow video frames for building training and validation sets, and the Petri dish images used for building the test set are shown. In particular, three frames from the in-flow video sequences related to CHP-134 and SK-N-SH are shown in (a) and (b), while two static images are shown in (c) (CHP-134 on the left and SK-N-SH on the right). A zoomed cell's view for each frame is shown on the right of holographic video frames (a) and (b) and Petri dish images (c).

Since the long-term goal of this study is to build a prototype of an in-flow cell tracking pipeline, for which real-time detection and segmentation of cells is required, we chose to automate the process of extracting the single cells that will be fed to the binary classifier by employing a Mask R-CNN [32]. Mask R-CNN is a state-of-the-art Convolutional Neural Network used for the task of instance segmentation, that is, it is able to detect the bounding boxes who delimit object instances belonging to a target class while also being able to output a mask which precisely segments the object inside each bounding box. In our case, we used a Mask R-CNN that was pre-trained on the COCO dataset [31]. We replaced the head of the network with a 2-class classification head in order to only predict cells vs. background. The Mask R-CNN was then trained to identify and segment cells (independently from their class) by using 200 cells manually extracted from the training set. The network was then run on the holographic frames in order to obtain candidate masks. The output masks were finally visually inspected to have a correct evaluation of the performance of the binary classifiers, which is the main focus of our study. In total, we extracted 983 CHP-134 cells and 918 SK-N-SH cells for the training set, 413 CHP-134 cells and 584 SK-N-SH cells for the validation set, and 301 CHP-134 cells and 207 SK-N-SH cells for the test set. The Mask

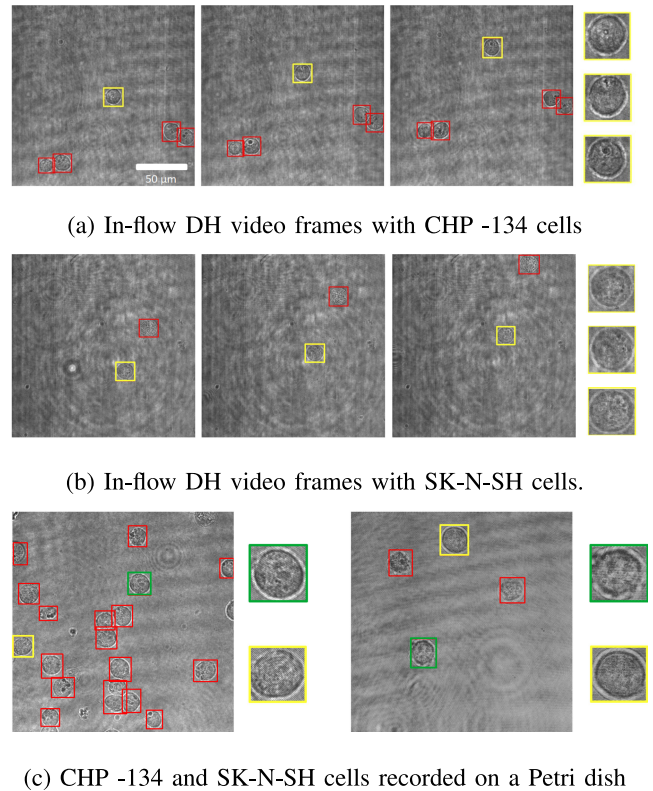


Fig. 3. (a) CHP-134 in-flow DH video sequence (5 cells); (b) SK-N-SH in-flow DH video sequence (2 cells); (c) CHP-134 (on the left, 19 cells) and SK-N-SH (on the right, 4 cells) cells recorded on a Petri dish. In (a) and (b) three frames from each video sequence are shown with an interval of 10 frames from each other (the leftmost is the first frame, while the rightmost is the last one. Frames are recorded at 285 ms intervals from each other). A zoomed cell view cropped from the holograms (a) and (b) is shown on the right of the frames (yellow boxes). In (c) a zoomed cell's view cropped from the Petri dish images is shown (yellow and green boxes).

R-CNN was fine-tuned for 40 epochs without validation. We used the Mask R-CNN code provided by [35].

C. DL Classifier

In this section, the DL architecture is shown. A binary classification model based on a CNN is applied to distinguish among cells of the CHP-134 and of the SK-N-SH lines. The CNN we used is an adaptation of the well-known LeNet-5 [34], as shown in Fig. 4. As it is a common practice with CNNs, the network is made of two main parts: a feature extractor and a classifier head. The input to the network has size 256×256 pixels, with each pixel being normalized in the range $[0, 1]$. The feature extractor is made of consecutive blocks of convolutional and max pooling layers, in an alternating fashion. All the convolutional blocks have a 3×3 kernel size, while all the pooling blocks perform downsampling using a window of size 2×2 . The 4 convolutional layers have respectively 32, 64, 128 and 128 filters. All the convolutional layers use a Rectified Linear Unit (ReLU) as activation function. The network head is instead composed of 2 fully-connected layers, the first comprising 512 neurons, while the last one has a single neuron with a sigmoid activation function, in order to obtain a probability class score

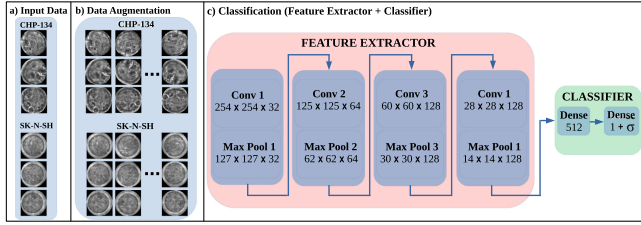


Fig. 4. The DL pipeline is summarized here. First (a), the cell masks are extracted from each holographic frame by using a Mask R-CNN, followed by a visual refinement. Data augmentation is then performed (b) by rotating each extracted cell by 10 degrees 36 times. This is useful to develop a rotation invariant binary classifier [37]. The training and validation sets are then used to train a LeNet-like CNN consisting of a feature extraction backbone and a classifier head (c). The backbone is made of a series of convolutional and max pooling layers. ReLu activation is used after each convolutional layer. The classifier head consists of two fully-connected layers, of 512 and 1 neurons respectively. A sigmoid activation function σ is applied to the last layer to obtain the class probability.

(if the value is less than 0.5, the cell is predicted as belonging to the CHP-134 class, otherwise as belonging to the SK-N-SH one).

To avoid overfitting, we adopted two main strategies. The first one is the use of data augmentation on the training set. Each cell from the training set was rotated 36 times by 10 degrees. This helps the network to compute rotational-invariant features during the training phase and prevents overfitting by obtaining a training set that is effectively 36 times larger than the original one. The second technique was the use of a dropout layer [36] between the two fully connected layers. The dropout layer randomly disables some of the connections between the two layers during training, forcing the network to be more robust to random noise and thus reducing overfitting to the training data.

The LeNet-like CNN was trained using binary cross-entropy as a loss function. The dropout factor was set to 0.5. We used the Adam optimization algorithm [38] with a learning rate of 0.0001. With this settings, the network was trained for 40 epochs with a batch size of 32 images, using the validation accuracy to perform early stopping, i.e. to choose the epoch which performed best on the validation set. We chose the weights at epoch 30 as the best weights from the training, as it is discussed in Section III. The LeNet-like CNN was implemented in Keras [39] on top of TensorFlow [40] in Python 3. The training was performed on a nVidia GeForce GTX 970 GPU with a 4 GB of VRAM.

D. Feature Based Classifier

In addition to the DL model, we employed two feature-based ML algorithms for the classification task. We show that it is possible to distinguish between two different cell lines looking at morphological/texture features extracted by each cell, as it is shown by [33]. First, 10 features are extracted from each cell image. Furthermore, a shallow MLP and a Logistic Regression (LR) are used to classify the cells looking at those extracted features.

1) *Feature Description*: The features extracted are the first order pixel statistics of standard deviation, kurtosis and skewness, second order texture statistics of contrast, correlation, homogeneity and energy, and the shape parameters of area,

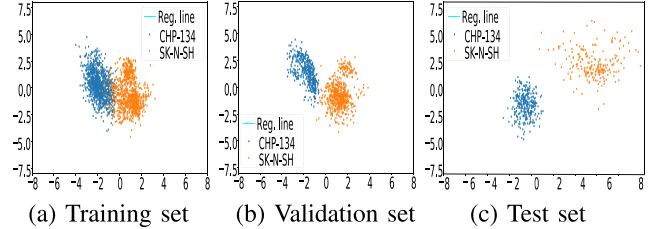


Fig. 5. 2D PCA decompositions over training set (a), validation set (b) and test set (c) are shown. The two lines cells (CHP-134 in orange and SK-N-SH in blue) are quasi perfectly separable. The first two principal components are shown here. The regression line learned by Logistic Regression is shown (cyan line).

eccentricity and perimeter. Before the training step, all the collected features are normalized by subtracting the mean of the whole datasets (training, validation and test sets) and then scaled to unit variance. The feature extraction is performed using Matlab [41] with the Image Processing Toolbox.

2) *Shallow Multilayer Perceptron*: Several architectures of the shallow MLP were tested, and the best one was selected by evaluating the performance on the training and validation sets. In particular, the selected network consists of an input layer of 10 neurons related to the 10 different features extracted from the cells. Then, one hidden layer with tanh activation function consisting of 32 neurons is added on top of the input. The output layer consists of 1 neuron and a sigmoid function is applied to obtain the class membership score. The network was trained using Adam [38] optimizer with a learning rate of 0.001. The MLP is implemented in Keras [39] on top of Tensorflow [40].

3) *Logistic Regression*: Looking at the 10 extracted features, it is possible to apply a logistic regression to separate cells from the two lines in the feature space using a hyperplane. We used the Principal Component Analysis (PCA) [42] algorithm and we show in Fig. 5 the two principal components related to the 10 extracted features and the regression line learned by the LR. After a fine-tuning step to obtain the best accuracy on training and validation sets, Newton was chosen as solver and no regularization was applied. PCA and LR are implemented using the Python library Scikit-learn [43].

III. EXPERIMENTAL RESULTS AND ROBUSTNESS ANALYSIS

ML and DL approaches outline different performances. In detail, the CNN learning curves over training and validation sets are shown in Fig. 6, box (a), suggesting that the network quickly reaches the 100% of accuracy on training and validation sets. In addition, the network reaches convergence very early and it does not overfit. The accuracy on the training and validation sets is 100%. CNN weights are chosen, to evaluate the network on the test set from the 30-th epoch, since it reaches a plateau on training and validation accuracy. The test accuracy is also 100%. In Fig. 6, box (b), the MLP learning curves over training and validation sets are shown. The MLP takes more epochs to reach the 100% of accuracy on both training and validation sets. The test accuracy is of 92.2% with only 38 classification errors by misclassifying SK-N-SH cells. Finally, the logistic regression

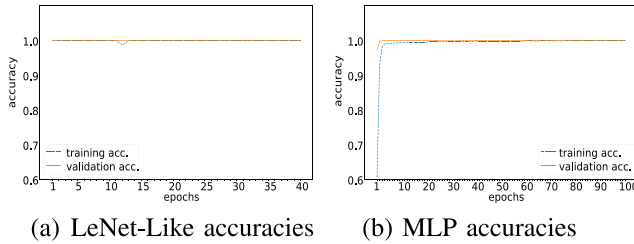


Fig. 6. Training accuracies related to LeNet-like CNN (a) and Shallow MLP (b) are shown. Both networks reach good accuracy value after few epochs. The CNN is trained on the holographic cell images, while the Shallow MLP is trained on the extracted features, listed in Section II-D1.

TABLE I
MEAN ACCURACY ON 10 DIFFERENT RANDOMLY CHOSEN SUB-DATASETS
CONTAINING 25% OF TOTAL CELLS

	TRAIN	VALIDATION	TEST
2D PCA + LR	0.963 ± 0.007	0.995 ± 0.002	0.706 ± 0.017
LR	1.000 ± 0.000	0.999 ± 0.001	0.892 ± 0.041
MLP	0.998 ± 0.002	0.999 ± 0.002	0.812 ± 0.025
CNN	1.000 ± 0.000	1.000 ± 0.000	0.996 ± 0.007

TABLE II
MEAN ACCURACY ON 10 DIFFERENT RANDOMLY CHOSEN SUB-DATASETS OF
TRAINING SET CONTAINING 50% OF TOTAL CELLS

	TRAIN	VALIDATION	TEST
2D PCA + LR	0.962 ± 0.004	0.996 ± 0.001	0.695 ± 0.016
LR	1.000 ± 0.000	0.999 ± 0.000	0.916 ± 0.013
MLP	0.998 ± 0.001	0.999 ± 0.001	0.848 ± 0.018
CNN	1.000 ± 0.000	1.000 ± 0.000	0.999 ± 0.001

TABLE III
MEAN ACCURACY ON 10 DIFFERENT RANDOMLY CHOSEN SUB-DATASETS OF
TRAINING SET CONTAINING 75% OF TOTAL CELLS

	TRAIN	VALIDATION	TEST
2D PCA + LR	0.965 ± 0.002	0.997 ± 0.000	0.702 ± 0.006
LR	1.000 ± 0.000	1.000 ± 0.000	0.924 ± 0.006
MLP	0.999 ± 0.001	1.000 ± 0.000	0.876 ± 0.007
CNN	1.000 ± 0.000	1.000 ± 0.000	1.000 ± 0.000

TABLE IV
ACCURACY ON THE WHOLE TRAINING DATASET

	TRAIN	VALIDATION	TEST
2D PCA + LR	0.967	0.997	0.701
LR	1.000	1.000	0.925
MLP	1.000	1.000	0.922
CNN	1.000	1.000	1.000

on the 10 extracted features reaches 92.5% of accuracy on the test set, while on the 2D PCA space it reaches 70.1%.

In order to evaluate the model robustness, we made 3 additional experiments for each method by varying the dimension of the training set from 25% to 75% of the original dataset. The mean accuracies reached by the proposed algorithms on these datasets and the standard deviation are shown in Table I, Table II and in Table III. ML and DL algorithms were trained 10 times on different randomly chosen sub-datasets. Finally, collecting all the data of the training set, in Table IV the performances reached by ML and DL models are shown. Although data in the 2D PCA space are well separable on training, validation and test sets, as shown in Fig. 5, the learned regression line

TABLE V

IN THIS TABLE, A QUALITATIVE COMPARISON BETWEEN THE CONVOLUTIONAL NEURAL NETWORK (CNN), MULTILAYER PERCEPTRON (MLP) AND LOGISTIC REGRESSION (LR) IS REPORTED. IN DETAILS, THE COMPARISONS ARE PERFORMED BY CONSIDERING SEVERAL FACTORS (I.E. REAL-TIME CONTEXTS, ROBUSTNESS TO THE LACK OF THE TRAINING DATA, FINE/COARSE INPUT IMAGE SEGMENTATION, ETC...). IN PARTICULAR FOR THE FIELD **FEATURE EXTRACTION**, EMBEDDED MEANS RELY ON AUTOMATICALLY EXTRACTED FEATURES. IN THE OTHER MODELS, THE FEATURES ARE EXTRACTED WITH SEVERAL PROCEDURES NOT INTEGRATED IN THE MODEL (EXTERNAL)

	CNN	MLP	LR
Real Time	YES	NO	NO
Dataset Subsampling Robustness	OPTIMAL	GOOD	GOOD
Supervised	YES	YES	YES
Coarse/fine input image segmentation	COARSE	FINE	FINE
Feature Extraction	EMBEDDED	EXTERNAL	EXTERNAL + PCA
Computational Resources	GPU	CPU/GPU	CPU
Output Result Understanding	NO	NO	YES

is unable to separate the two cell lines on the test set, since the LR is trained on the training and validation sets. This is because the test samples follow a different distribution than in the training/validation sets. The LR and PCA reaches an accuracy of 70,1% on the whole training dataset. LR increases its accuracy considering 10 features (92,2%). However, both LR and MLP have worse performances using smaller training datasets. Finally, CNN obtains the best accuracy on the test set in all the cases, showing robustness to the lack of data in the training set. In Table V, a comparison between proposed models is shown.

Another test was performed eliminating the manual artifacts removal step from the whole procedure in order to verify proposed models' real-time constraints. In this case, the Mask RCNN does not return perfect binary masks, but it gives in output the cell bounding boxes which are taken *as they are* to feed the CNN. The previous training set of the CNN is divided into training and validation for the Mask RCNN, while the validation set and the test set of the CNN in the previous experiments are now the test sets for in flow and Petri dish images, respectively. This was made to reduce the bias and overfitting risks of the MASK RCNN + CNN pipeline. In particular, the Mask R-CNN returns in output 1.41% of False Positives and 0.16% of False Negatives for the in-flow test images, and 0.99% of False Positives and 4.75% of False Negatives on the Petri dish test images. Furthermore, the trained CNN reaches 100% of accuracy on training, validation, and test set once the extracted False Positives are removed by the datasets. This evidence combined with the generalizing power of a CNN leads us to consider cell lines classification not affected by the bounding boxes' inclusion procedure. Instead, the other algorithms need a fine input image segmentation and a feature extraction step. In general, the training of CNN needs high computational resources based on GPUs. In our case, LeNet-like CNN fits also on personal computer with low-budget GPUs (like GTX 970- 4 GB of VRAM).

IV. DISCUSSION AND CONCLUSION

In this paper, ad-hoc learning approaches for reliable classification of biological samples' raw recorded digital holograms are investigated. Even if there are similar learning approaches

in literature [24]–[29], to the best of our knowledge, for this specific type of data, the learning strategies proposed in this paper were never applied and compared. In detail, our analyses are focused on two neuroblastoma cell lines. Nevertheless, once new data are available, our intention is to extend these analyses on several biological samples. Our work demonstrates that a highly phenotyping accuracy is achievable even with raw data, thus avoiding the phase retrieval reconstruction process. Our Mask-R-CNN outputs (bounding box/mask extraction) combined with LeNet-like CNN based classification reaches the 100% of accuracy, while MLP and Logistic Regression (on binary mask inputs) reach a classification accuracy on test set of 92.2% and 95.5%, respectively. In addition, it is proved that the CNN classification accuracy is robust with respect the bounding boxes' inclusion procedure. In detail, in this work, the reached classification accuracy, combined with robustness testing, allows for the separation of CHP-134 and SK-N-SH cell lines with high precision and reliability. Our research show that MLP and Logistic Regression need fine input image segmentation for a correct classification. In these cases, despite the real-time constraints, this is only possible with a manual removal of the artifacts or with non-real-time traditional algorithms. As it is shown in [44]–[46], the non-trainable segmentation algorithms need a parameter optimization, which depends on image quality and cell clusters. Furthermore, they need a cell identification to distinguish artifacts. Instead, DL has been used in many types of applications, ensuring reliability and efficiency, especially in image processing/classification tasks. In conclusion, this paper shows that Mask R-CNN and LeNet-like CNN applied to two cell lines could be used in real-time classification during biological samples holographic acquisition. This is possible in the case of diagnostic strategies based on microfluidic systems, such as the identification of CTCs within blood samples and where high-throughput is needed [21]; Furthermore, CNNs applied to this particular type of data may allow interesting future research results by leveraging the advances of the Multiple Object Tracking (MOT) [47] on holographic video streams. In fact, it is well known that CNNs are able to correctly identify hundreds of objects in a single frame [48].

Finally, it is worth remarking that the possibility to solve classification problems by using digital holograms as input to a learning-based classifier has been recently explored in [26]–[28] but our method is the only one that uses holograms of flowing and rotating cells for the training and static recording for the testing. Moreover, the phenotyping of neuroblastoma cells is addressed for the first time in this modality. Although our approach completely skips the holographic reconstruction process, the use of DH imaging is decisive to achieve the above remarkable results. In fact, since both phase and amplitude information are encoded within a hologram, this pattern is more informative than a diffracted pattern obtainable with a single beam [49]. Moreover, using an interferometric system is advantageous also for post-classification tasks. Indeed, once a cell is classified and associated to a certain population, it could be of interest to achieve additional morphometric information a posteriori (e.g., its dry mass, biovolume, thickness, shape information). Within this scope, retrieving the phase of the object wavefront

is necessary. We believe this pioneering study has an impact in the biomedical field of liquid biopsy by paving the way for an unlabeled methodology to identify heterogeneous CTC populations in body fluids without specific antigenic markers available.

V. DISCLOSURES

The authors declare no conflicts of interest.

REFERENCES

- [1] P. Ferraro, A. Wax, and Z. Zalevsky, *Coherent Light Microscopy*, Berlin, Germany: Springer, vol. 46, 2011.
- [2] Y. K. Park, C. Depeursinge, and G. Popescu, "Quantitative phase imaging in biomedicine," *Nat. Photon.*, vol. 12, pp. 578–589, 2018.
- [3] V. Bianco *et al.*, "Microplastic identification via holographic imaging and machine learning," *Adv. Intell. Syst.*, vol. 2, no. 2, 2020, Art. no. 1900153.
- [4] T. J. H. GoH. KimByeon, and S. J. Lee, "Machine learning-based in-line holographic sensing of unstained malaria-infected red blood cells," *J. Biophotonics*, vol. 11, no. 9, 2018.
- [5] A. V. Belashov *et al.*, "In vitro monitoring of photoinduced necrosis in hela cells using digital holographic microscopy and machine learning," *J. Opt. Soc.*, vol. 37, pp. 346–352, 2020.
- [6] R. Strack, "Deep learning in imaging," *Nat. Methods*, vol. 16, no. 1, pp. 17–17, 2019.
- [7] Y. Jo *et al.*, "Quantitative phase imaging and artificial intelligence: A review," *IEEE J. Sel. Topics Quantum Electron.*, vol. 25, no. 1, pp. 1–14, Jan.-Feb. 2019.
- [8] E. Moen, D. Bannon, T. Kudo, W. Graf, M. Covert, and D. Van Valen, "Deep learning for cellular image analysis," *Nature Methods*, pp. 1–14, 2019.
- [9] Q. Wang, S. Bi, M. Sun, Y. Wang, D. Wang, and S. Yang, "Deep learning approach to peripheral leukocyte recognition," *Plos One*, vol. 14, no. 6, 2019, Art. no. e0218808.
- [10] L. L. Zeune *et al.*, "Deep learning of circulating tumour cells," *Nat. Mach. Intell.*, vol. 2, no. 2, pp. 124–133, 2020.
- [11] M. Xu, D. P. Papageorgiou, S. Z. Abidi, M. Dao, H. Zhao, and G. Em Karniadakis, "A deep convolutional neural network for classification of red blood cells in sickle cell anemia," *PLoS Comput. Biol.*, vol. 13, no. 10, 2017, Art. no. e1005746.
- [12] G. Litjens *et al.*, "Deep learning as a tool for increased accuracy and efficiency of histopathological diagnosis," *Sci. Report.*, vol. 6, 2016, Art. no. 26286.
- [13] A. Krizhevsky, I. Sutskever, and G. E. Hinton, "Imagenet classification with deep convolutional neural networks," in *Proc. Adv. Neural Infor. Process. Syst.*, 2012 pp. 1097–1105.
- [14] C. L. Chen *et al.*, "Deep learning in label-free cell classification," *Sci. Report.*, vol. 6, 2016, Art. no. 21471.
- [15] Y. Rivenson, Y. Wu, and A. Ozcan, "Deep learning in holography and coherent imaging," *Light: Sci. Appl.*, vol. 8, no. 1, pp. 1–8, 2019.
- [16] P. Memmolo *et al.*, "Recent advances in holographic 3 d particle tracking," *Adv. Opt. Photon.*, vol. 7, no. 4, pp. 713–755, 2015.
- [17] S. K. Mohammed, L. Bouamama, D. Bahloul, and P. Picart, "Quality assessment of refocus criteria for particle imaging in digital off-axis holography," *Appl. Opt.*, vol. 56, no. 13, pp. F 158–F166, 2017.
- [18] P. Memmolo, V. Renó, E. Stella, and P. Ferraro, "Adaptive and automatic diffraction order filtering by singular value decomposition in off-axis digital holographic microscopy," *Appl. Opt.*, vol. 58, no. 34, pp. G 155–G161, 2019.
- [19] Y. Rivenson, Y. Zhang, H. Günaydn, D. Teng, and A. Ozcan, "Phase recovery and holographic image reconstruction using deep learning in neural networks," *Light: Sci. Appl.*, vol. 7, no. 2, pp. 17141–17141, 2018.
- [20] Z. Ren, Z. Xu, and E. Y. M. Lam, "End-to-end deep learning framework for digital holographic reconstruction," *Adv. Photon.*, vol. 1, no. 1, 2019, Art. no. 016004.
- [21] L. Miccio *et al.*, *Perspectives on Liquid Biopsy for Label-Free Detection of "Circulating Tumor Cells" Through Intelligent Lab-on-Chips.*, VIEW, 2020.
- [22] F. Merola *et al.*, "Tomographic flow cytometry by digital holography," *Light: Sci. Appl.*, vol. 6, no. 4, pp. e16241–e16241, 2017.
- [23] M. M. Villone *et al.*, "Full-angle tomographic phase microscopy of flowing quasi-spherical cells," *Lab Chip*, vol. 18, no. 1, pp. 126–131, 2018.

- [24] B. Javidi, S. Rawat, S. Komatsu, and A. Markman, "Cell identification using single beam lensless imaging with pseudo-random phase encoding," *Opt. Lett.*, vol. 41, no. 15, pp. 3663–3666, Aug. 2016.
- [25] G. Satat, M. Tancik, O. Gupta, B. Heshmat, and R. Raskar, "Object classification through scattering media with deep learning on time resolved measurement," *Opt. Exp.*, vol. 25, no. 15, pp. 17466–17479, Jul. 2017.
- [26] S. Jiao, J. Feng, Y. Gao, T. Lei, Z. Xie, and X. Yuan, "Optical machine learning with incoherent light and a single-pixel detector," *Opt. Lett.*, vol. 44, no. 21, pp. 5186–5189, Oct. 2019.
- [27] H. H. Lam, P. W. M. Tsang, and T.-C. Poon, "Ensemble convolutional neural network for classifying holograms of deformable objects," *Opt. Exp.*, vol. 27, no. 23, pp. 34050–34055, Nov. 2019.
- [28] B. Schneider, G. Vanmeerbeek, R. Stahl, L. Lagae, and P. Bienstman, "Using neural networks for high-speed blood cell classification in a holographic-microscopy flow-cytometry system," *Proc. SPIE 9328, Imag., Manipulation, Anal. Biomolecules, Cells, Tissues XIII*, Mar. 2015 <https://doi.org/10.1117/12.2079436>.
- [29] S. Kim *et al.*, "Deep transfer learning-based hologram classification for molecular diagnostics," *Sci. Rep.*, vol. 8, no. 12, 2018.
- [30] S. Jiao, Y. Gao, J. Feng, T. Lei, and X. Yuan, "Does deep learning always outperform simple linear regression in optical imaging?" *Opt. Exp.*, vol. 28, no. 3, pp. 3717–3731, Feb. 2020.
- [31] T. Lin *et al.*, "Microsoft coco: Common objects in context," in *Proc. Europ. Conf. Comput. Vis.*, 2014, pp. 740–755.
- [32] K. He, G. Gkioxari, P. Dollár, and R. Girshick, "Mask r-cnn," in *Proc. IEEE Int. Conf. Comput. Vis.*, 2017, pp. 2961–2969.
- [33] V. K Lam, T. C Nguyen, B. M Chung, G. Nehmetallah, and C. B Raub, "Quantitative assessment of cancer cell morphology and motility using telecentric digital holographic microscopy and machine learning," *Cytometry Part*, vol. 93, no. 3, pp. 334–345, 2018.
- [34] Y. LeCun, L. Bottou, Y. Bengio, and P. Haffner, "Gradient-based learning applied to document recognition," *Proc. IEEE IRE*, vol. 86, no. 11, pp. 2278–2324, 1998.
- [35] W. Abdulla, Mask R-Cnn for Object Detection and Instance Segmentation on Keras and TensorFlow, 2017, [Online]. Available: https://github.com/matterport/Mask_RCNN
- [36] N. Srivastava, G. Hinton, A. Krizhevsky, I. Sutskever, and R. Salakhutdinov, "Dropout: A simple way to prevent neural networks from overfitting," *J. Mach. Learn. Res.*, vol. 15, no. 1, pp. 1929–1958, 2014.
- [37] F. Quiroga, F. Ronchetti, L. Lanzarini, and A. F Bariviera, "Revisiting data augmentation for rotational invariance in convolutional neural networks," in *Proc. Int. Conf. Modell. Simulation Manage. Sci.*, 2018, pp. 127–141.
- [38] D. P Kingma and J. Ba, "Adam: A method for stochastic optimization," 2014, *arXiv:1412.6980*.
- [39] F. Chollet *et al.* Keras, 2015, [Online]. Available: <https://keras.io>
- [40] M. Abadi *et al.*, "Tensorflow: Large-scale machine learning on heterogeneous distributed systems," 2016, *arXiv:1603.04467*.
- [41] MATLAB. version 9.8.0.1396136 (R2020a). MathWorks Inc, Natick, Massachusetts, 2020.
- [42] K. Pearson and F. R. S. Liii, "On lines and planes of closest fit to systems of points in space. the london, edinburgh, and dublin philosophical magazine," *The London, Edinburgh, and Dublin Philosophical Magazine and Journal of Science*, vol. 2, no. 11, pp. 559–572, 1901.
- [43] F. Pedregosa *et al.*, "Scikit-learn: Machine learning in python," *J. Mach. Learn. Res.*, vol. 12, pp. 2825–2830, 2011.
- [44] T. Vicar *et al.*, "Cell segmentation methods for label-free contrast microscopy: Review and comprehensive comparison," *BMC Bioinf.*, vol. 20, no. 12, 2019.
- [45] Z. Wang and H. Li, "Generalizing cell segmentation and quantification," *BMC Bioinf.*, vol. 18, no. 12, 2017.
- [46] Z. Wang, "Cell segmentation for image cytometry: Advances, insufficiencies, and challenges," *Cytometry Part*, vol. 95, no. 7, pp. 708–711, 2019.
- [47] G. Ciaparrone, F. Luque Sánchez, S. Tabik, L. Troiano, R. Tagliaferri, and F. Herrera, "Deep learning in video multi-object tracking: A survey," *Neurocomputing*, vol. 381, pp. 61–88, Mar. 2020.
- [48] P. Dendorfer *et al.*, Mot20: A Benchmark for Multi Object Tracking in Crowded Scenes, 2020.
- [49] O. Mudanyali *et al.*, "Compact, light-weight and cost-effective microscope based on lensless incoherent holography for telemedicine applications," *Lab. Chip*, vol. 10, pp. 1417–28, Jun. 2010.

Mattia Delli Priscoli received the B.Sc. and M.Sc. degrees in computer engineering from the University of Salerno, Fisciano, Italy. He is currently working toward the Ph.D. degree in big data management from the University of Salerno, Fisciano, Italy. He is working on several deep learning tasks, like microscopy image processing and advanced neural network training strategies. His research interests include artificial and computational intelligence, deep learning, and image processing.

Pasquale Memmolo (Senior Member, IEEE) received the Ph.D. degree in electronic and telecommunication engineering from the Università degli Studi di Napoli "Federico II," Naples, Italy, in 2012. From 2012 to 2015, he was a Postdoctoral with the Center for Advanced Biomaterials for Health Care@CRIB, Italian Institute of Technology, Italy. In 2016, he joined the Institute of Applied Science and Intelligent Systems "E Caianiello" (ISASI), National Research Council of Italy and in the early of 2020, he got the Senior Researcher position. His main research interests includes the field of computational microscopy, ranging within topics, such as digital holography, optical engineering, optical tomography, microfluidics, lab-on-a-chip, computer vision, and machine learning.

Gioele Ciaparrone received the B.Sc. and M.Sc. degrees in computer science from the University of Salerno, Italy, in 2015 and 2017, respectively. He is currently working toward the Ph.D. degree in big data management from the University of Salerno, Italy. His current research interests include machine learning, deep learning and computer vision, in particular regarding image, and video analysis.

Vittorio Bianco received the M.S. degree (*cum laude*) in telecommunications engineering from the University "Federico II" of Naples, Naples, Italy, and the Ph.D. degree in materials and structures engineering, in 2016. In 2017, he was a Postdoctoral with the University of California, Los Angeles (UCLA), USA, working in the field of lensless inline digital holography. In 2011, he worked with the German Aerospace Centre, Munich, Germany, in the fields of SAR interferometry and tomography. Since 2012, he has been with the Italian National Research Council in the fields of digital holography, optics and image processing, computational microscopy, optical systems engineering, microfluidics, diagnostics and environmental monitoring. He has coauthored more than 110 works in his fields of expertise. He was the recipient of the IEEE Best Doctoral Thesis in Optoelectronics 2016 Award.

Francesco Merola received the M.S. degree in physics (*cum laude*) and the Ph.D. degree in fundamental and applied physics, from University of Napoli "Federico II," Italy, in 2006 and 2009, respectively. In 2007, he joined the National Council of Research (CNR) in Napoli, where he is currently a Permanent Researcher with the Institute of Applied Science & Intelligent Systems (ISASI). He has published several works with IEEE Society, among which the highly cited "F. Merola *et al.* Proc. of the IEEE 103, 192-204 (2015)," Invited for the Special Issue Global Healthcare (I.F.=10.252). His research interests include Optical Tweezers, Digital Holographic Microscopy, Tomography and Lab-On-Chip technology and other intersets covered the circulating tumor cells identification and 3D imaging by in-flow tomography as a liquid biopsy, microplastics analysis in marine samples and identification/counting by digital holography and machine learning techniques; patterning and self-assembling of liquid crystal nanodrops, deposited or embedded in polymer-coated micro-engineered substrates. In this regard, he is involved in two funded projects (PRIN "MORFEO" - MORphological biomarkers For Early diagnosis in Oncology and PON "SiRiMaP" - Innovative Detection Systems for the Marine Plastic Pollution Monitoring, Recovery and Recycling). His current interests includes analysis of seawater contamination from both microplastics and heavy metals, studying the impact of such pollutants on fitoplankton by non-invasive optical techniques. He has authored or coauthored more than 100 papers and proceedings on International Journals, and four book chapters. He has been speaker in about 20 International Conferences (some of which as Invited). He is Referee of international Journals as IEEE Journal of Display Technology, Biomedical Optics Express, Scientific Reports, ACS Photonics. He received awards from OSA (Optical Society of America) and from Light: Science & Applications (Nature Group) for two outstanding papers, and from SIF (Italian Society of Physics) as Young graduated in Physics for his master's thesis.

Lisa Miccio received the physics degree from the University of Naples “Federico II”, Italy and the International Ph.D. degree from the University of Florence, Firenze, Italy, in 2006 and 2010, respectively. She has been a Visiting Scholar with Universidad Complutense, Madrid, Spain during the Ph.D. school and with the University of Munster, Germany in the framework of Horizon 2020 cost action. She is currently a Staff Researcher with Italian National Research Council Institute of Applied Sciences and Intelligent Systems (CNR-ISASI). She is physicist working in Applied Optic field. Her research interests include quantitative phase microscopy and tomography. Main research activities concern the investigation of label-free approaches for imaging in biomedical application, industrial inspection, and cultural heritage. She has skills in developing optical arrangements operating with coherent and low-coherent light. She has expertise in image processing for quantitative phase-contrast evaluations. She is also involved in developing new-engineered interfaces for biomaterial manipulation. She has authored or coauthored more than 70 peer-review papers, she attended more than 50 international conferences and she is a Supervisor of Ph.D. students and research fellows.

Francesco Bardozzo received the B.Sc. and M.Sc. degrees with honor’s in computer science, with theses in artificial and computational intelligence, from the Faculty of Sciences, University of Salerno, Fisciano, Italy. He is currently working toward the Ph.D. degree in big data management, University of Salerno, Fisciano SA, Italy. His research interests include artificial and computational intelligence, machine learning, deep learning and computational biology with special stress in multi-omic oscillations, soft tissue reconstruction, and neuroimaging.

Daniele Pirone received the B.S. and M.S. degrees in biomedical engineering from the University of Naples “Federico II, Napoli, Italy, in 2017 and 2019, respectively, where he is currently working toward the Ph.D. degree in “Information and Communication Technology for Health (ICTH) XXXV cycle,” from the University of Naples “Federico II. He is a Research Fellow with the Italian National Research Council-Institute of Applied Sciences and Intelligent Systems (CNR-ISASI). His research interests include signal and image processing, digital holography in microscopy, quantitative phase imaging and phase contrast tomography, mainly for biomedical applications.

Martina Mugnano received the Graduate degree in health biotechnologies with thesis on “3D skin model production in-vitro” and completed the Second Cycle degree in medical biotechnology with a dissertation on “Identification and characterization of a novel transcription factor involved in osteoblast differentiation and the Ph.D. degree in “engineering of industrial products and processes” with a thesis on “Optical manipulation and advanced analysis of cells using an innovative optofluidic platform”, from the University of Naples Federico II, Napoli, Italy, studying the interaction between smart materials such as lithium niobate crystal and diverse biological samples and includes bio-imaging studies of the interaction of light and cells under the supervision of Dr. Pietro Ferraro, with ISASI - Institute of Applied Science and Intelligent Systems (CNR - National Research Council of Italy). He has authored or coauthored more than 52 scientific publications in international journals and conference proceedings. He is currently working on SensApp a FET-open project funded by the Horizon 2020 funding programmes of the European Commission. SensApp aims at developing a super-sensor system that will be able to detect the Alzheimer’s disease biomarkers in human plasma, for an early diagnosis of Alzheimer’s disease.

Flora Cimmino was born in Naples, Italy on the 8th of March 1981. She received the Ph.D. degree in molecular oncology and postgraduate education in Medical Genetics residency school, from the University of Naples Federico II, Napoli, Italy. She has been a Visiting Researcher with the University of Essen-Duisburg, Duisburg, Germany for one year and since 2013, she is a Researcher with Fondazione Umberto Veronesi. She is a Senior Postdoc with an extensive experience in cancer genetic/genomic field. Her research interest focuses on coding and non-coding somatic variants identification by the use of high-throughput methodology (WES, WGS) and CRISPR-Cas9 editing. In the last years she is extending her scientific interest in liquid biopsy field, particularly ctDNA sequencing from plasma of adult and pediatric cancer patients.

Mario Capasso was born in Napoli, Italy, in 1977. He received the B.S. and M.S. degrees in biotechnologies from the University of Naples Federico II, Napoli, Italy, in 2001 and the Ph.D. degree in molecular medicine from the University of Foggia, Foggia, Italy, in 2007. From 2001 to 2007, he was a Research Assistant with the Human Genetics Laboratory, CEINGE institute University of Naples Federico II, Napoli, Italy. From 2007 to 2008, he was a Postdoc with The Children Hospital of Philadelphia. From 2010 to 2018, he was an Assistant Professor in medical genetics with the University of Naples Federico II. Since 2018, he has been an Associate Professor in medical genetics with the University of Naples Federico II. He has authored more than 80 articles. He has the expertise in bioinformatics and in vitro functional analysis of genomic data obtained by diverse methodological approaches such as SNP array, qPCR, gene expression array, and next generation sequencing. His research focuses translational genomics in pediatric cancers. He was the recipient of the Guido Paolucci International Award of Geomagnetism and Aeronomy Young Scientist Award for the Best Scientific Article in Pediatric Oncology in 2010.

Achille Iolascon received the Graduate degree in medicine and surgery from the University of Naples “Federico II”, Napoli, Italy, and the postgraduate degree in pediatrics and oncology, and a Ph.D. degree in Pediatrics, in 1981, 1985, and 1986, respectively. Since 1983, he has been working in the field of rare anemias and he gradually gained international recognition in this field. Using continuously renewed methods in molecular biology and in medical genetics, he characterized a large number of previously unknown genes and mutations: SPTA1, ANK1, AE1, SEC23B, ABCB6, and PIEZO1. He is currently Full Professor of Medical Genetics with the University of Naples “Federico II”, the Director of the Post-graduate School of Medical Genetics, University Federico II of Naples, the Head of the Medical Genetics Unit, Federico II University Hospital, and PI of a research group at CEINGE- Advanced Biotechnologies, Naples, Italy. His research group is currently an international reference group for genetics of rare hemolytic anemias, either due to hyporegenerative defects or RBCs membrane defects. He has also been the President of Italian Society of Human Genetics since 2019.

Pietro Ferraro (Senior Member, IEEE) received the graduate degree (*cum laude*) in physics from the University of Naples “Federico II,” Naples, Italy, in 1987. He founded the Institute of Applied Sciences and Intelligent Systems of CNR and has been the Director from 2014 to 2019. He is the Research Director with ISASI. He has authored or coauthored more than 320 articles in peer-reviewed journals and more than 200 conference papers. His research interests include digital holography, microscopy, laser interferometry, lithography, ferroelectric crystals for photonic applications, and lab-on-a-chip for biomedical applications. He was Elected Fellow of SPIE in 2008 and a Fellow of the Optical Society of America in 2010. In 2020, he received the SPIE Dennis Gabor Award.

Roberto Tagliaferri (Senior Member, IEEE) has had courses in computer architectures, artificial and computational intelligence, and bioinformatics for computer scientists and engineers, and biologists. He is currently a Full Professor in Computer Science with the University of Salerno, Fisciano, Italy. He has been a Co-Organizer of international workshops and schools on neural nets, computational intelligence, and bioinformatics. He has authored or coauthored more than 150 articles in peer-reviewed journals and conferences. His research interests include computational intelligence models and applications in the areas of astrophysics, biomedicine, bioinformatics, and industrial applications. He has been Co-Editor of special issues on international journals and proceedings of international conferences.